Cyclo-nonstationary analysis for bearing fault identification based on instantaneous angular speed estimation

Edgar F. Sierra-Alonso[1,2] Jerome Antoni[1] German Castellanos-Dominguez[2]
[1]Laboratoire Vibrations Acoustique, Univ Lyon, INSA-Lyon,
LVA EA677, F-69621, Villeurbanne, France
edgar-felipe.sierra-alonso@insa-lyon.fr
[2]Signal Processing and Recognition Group, Universidad Nacional de Colombia,
Km 9 way to magdalena, Manizales Caldas, Colombia

Abstract

Rolling Element Bearings (REB) are present in most of the rotating machines being the ones in charge of supporting the charge of the shaft, being the cosntant charge of the shaft a reason to make the REB prone to fail. Failures under real conditions such as variable speed/load are a subject of interest in the state of the art in digital signal processing of vibration signals, lastly, defined as a cyclo-nonstationary process due to the intrinsic cyclic behaviour of the REB and the nonstatinarity introduced by the variations of the Instantaneous Angular Speed (IAS). The most direct approach to deal with a REB failure under time-varying IAS, is to compensate the IAS transforming the vibration signal to the angular domain, then highlight the cyclo-stationary part of the signal in the angular domain. To obtain the IAS, the direct approach is to measure the IAS via an encoder to obtain the so-called tachometer signal, to place an encoder usually requires a modification of the machine. In cases where it is not possible, the IAS could be extracted directly from the vibration signal. To extract the IAS from a vibration signal is a hard task due to to the low Signal to Noise Ratio (SNR); consequently, a short-time approach methodology robust to noise for IAS estiamtion termed, Short Time Non-Linear Least Squares (STNLS) estimation is proposed. However, even with the IAS to identify the failure requires an additional step that is to highlight the impulsive behaviour, several techniques in the literature makes use directly or indirectly of the Spectral Kurtosis (SK) to highlight impulsive behaviour. The SK is designed to work under small variations of the IAS, even when the variation on the IAS could be compensated through the transformation to the angular domain; there are components angle-variant like the transfer function, that could mask the impulsive components. Thus, a short-angle method based on the SK named Short Time/Angle Spectral Kurtosis (STSK) is introduced. The STSK method is compared with the traditional approach outperforming in both numerical an a challenging case study of an aircraft engine. Similarly, the STNLS is tested on a numerical database for robustness to noise and in the real signal showing a Mean Square Error bellow 5×10^{-3}.

1 Introduction

The Instantaneous Angular Speed (IAS) alongside the acceleration data is one of the most important parameters to measure in condition monitoring. In our case study, to identify a rolling element bearing (REB) failure under variable speed is mandatory to deal with highly non-stationary conditions, mainly caused by the variation of the speed, that modifies the underlying cyclo-stationary process. Due to for REB failures the failure frequency is a function of the angular speed, it is impossible to identify a failure without this parameter [1]; consequently, the IAS is one of the most important parameters to measure. However, the speed measurement is sensitive to disturbances like loss of samples or artifacts[2]. Alternatively, the IAS can be extracted directly from the vibration signal, where this is the most challenging situation. Due to the multi-component nature of the signal, where different families of harmonics may coexist, alongside with the interaction between the orders and the structural resonances of the machine, and the low Signal to Noise Ratio (SNR) where noise comprises any component in the signal which is not of direct interest for the analysis [3]. The importance of the IAS measurement/extraction is of the continuous interest in the literature for REB fault detection under variable IAS; the subject was recently addressed in [4] where is concluded that the uniform angular re-sampling using

the IAS profile is the most common pre-process to identify A REB failure under variable speed. As it is expected to deal with low SNRs, the proposed approach must be robust. For such a reason, it is proposed the use of a Short-Time Non-Linear Least Squares (STNLS) method to estimate the IAS, assuming that a signal is stationary in a short-time segment.

A mandatory pre-process when dealing with vibration signals under variable speed is to transform the signal into the angular domain. The signal is transform throughout the uniform angular re-sampling a technique that transform a signal vibration signal in order to have the same amount of samples per rotation [5]. Nevertheless, as stated in [3] a vibration signal is affected by noise, where the noise is understood as any component in the signal which is not of direct interest for the analysis. Such noise is not entirely removed by any method even by the Spectral Kurtosis (SK). The SK is a low computational and effective tool to highlight impulsive behaviour in a seemly constant speed scenario, like in the case of a cyclo-stationary process [6]. Besides the SK, the traditional approach is to apply the envelope analysis to an angular re-sampled vibration signal [1]; however, the traditional approach is effective only in the case of small fluctuations[7]. Therefore, there is a need to develop more robust, automatic algorithms, suitable for different operating conditions, which leads to the relaxation of the constraint of the constant speed [8]. Recently, [9] proposed an extension of the cyclic spectral correlation for a time-varying speed scenario. However, it is assumed that time-dependent components are independent of the operating speed, which may be acceptable for modest speed variations; thus, its compensation constitutes an emerging field of investigation.

For such a reason, to highlight a REB failure under variable speed under highly non-stationary conditions. It is proposed in the present work a parametric methodology named STNLS for IAS estimation short-time based, and after the angular re-sampling by means of the IAS. It is proposed a REB highlight method that makes use of a Short-Time/Angle frequency 2D filter based on the Spectral Kurtosis (STSK), given that a signal it is expected to be stationary regardless the domain (time or angle) if a window small enough is considered. The robustness of the STNLS method is tested in a simulated signal contaminated with different levels of two different types of noise (pink and white). Finally, the STNLS and STSK are successfully applied in a case study of an aircraft engine publicly available in[4].

2 Theoretical background

This section intrudes the theory about the IAS estimation and the REB failure detection. First, a multi-harmonic model is introduced, and grounded in that model it is proposed the STNLS IAS estimation procedure. Likewise, a model for a REB failure as a superposition of impulses under constant IAS is introduced to numerically prove the proposed STSK filter to highlight a cyclo-stationary process. To do so, the influence of the time-varying IAS on the signal with respect to the traditional model, can be seen as a change of variable, and its compensation is the traditional Computed Order Tracking (COT), with that model in mind it is introduced a Short-Time/Angle Spectral Kurtosis (STSK) filter.

2.1 IAS estimation

The IAS of a given shaft is defined as the fundamental frequency of a multi-harmonic sum measured in a time interval $\mathbf{T} = [t_1, t_2] \subset \mathbb{R}^+$ with a duration $T = t_2 - t_1$. Let us define $\{f_{i,k}(t)\}_{i,k=1}^{I,K}$ such that $f_{i,k}(t) \in \mathbb{R}^+$ is the set of instantaneous frequencies of interest[1], where $\{i,k\}$ denotes the i-th fundamental frequency of the k-th reference shaft. In general a vibration signal $x(t) \in \mathbb{C}$ for the IAS extraction task is modelled as:

$$x(t) = \sum_{i,k=1}^{I,K} a_{i,k}(t) e^{j\phi_{i,k}(t)} + \eta(t) \tag{1}$$

where $a_{i,k}(t) \in \mathbb{C}$ is the time-varying amplitude for the i-th harmonic and the k-th harmonic family, the Instantaneous Angular Displacement[2] $\phi_{i,k}(t) \in \mathbb{R}^+$ is defined as:

[1] the Instantaneous Angular Speed is an Instantaneous Frequency $f_{i,k}(t)$ for which the index $i = 1$, and it is in rad.

[2] the angular displacement is related to the physical phenomenon of interest but in Signal Processing in general it is the phase of the signal.

$$\phi_{i,k}(t) = \int_{t\in\mathbf{T}} f_{i,k}(t)dt \tag{2}$$

$$f_{i,k}(t) = if_{1,k}(t) \tag{3}$$

and $\eta(t) \sim \mathcal{N}(\mu, \sigma^2)$ is stationary Additive White Gaussian Noise (AWGN) with $\mu = 0$. The reader should notice that in practice the noise $\eta(t)$ comprises any component that is not of interest, but as the AWGN is the worst and most common noise that can be found on a signal, the noise in the Eq. (1) is modelled as such. Consequently, the stochastic signal $x(t)$ has two parts: the sum that is the deterministic part, and the stochastic part modelled as AWGN. Adding as a restriction that the signal has a dominant multi-harmonic family, the vibration signal is modelled as a signal from a machine with only one shaft, consequently, the Eq. (1) is rewritten as:

$$\hat{x}(t) = \sum_{i=1}^{I} a_i(t)e^{j\phi_i(t)} + \eta(t) \tag{4}$$

where $\phi_i(t) = i\phi_{1,1}(t)$ and $a_i(t) = a_{i,1}(t)$. Note that in general $\hat{x}(t) \neq x(t)$, using $\hat{x}(t)$ it can be estimated $\hat{f}_1(t)$ with a Non-linear Least Squares estimation procedure. As in theory $x(t)$ is a *quasi-stationary signal* of real domain and complex range[3], it is assumed that in a short-time window the stochastic signal is stationary, for such a reason a Short-Time Non-Linear Least Squares (STNLS) estimation procedure is studied in the present work.

2.1.1 Short-time Non-Linear Least Squares IAS estimation

As the signal $x(t)$ is said to be quasi-stationary on a short-time interval. Thus, the proposed STNLS procedure is the traditional Non-Linear Least Squares estimation, but, applied to all the obtained short-time segments through a sliding window [4]. As $x(t)$ is quasi-stationary if the interval in which $t \in [t_c - t_T/2, t_c + t_T/2] \subset \mathbb{R}^+$ is small enough, for convenience let us define a short-time signal in discrete time notation. A signal in discrete time is defined as $x[n] = x(n\Delta t)$ for a given sampling time $\Delta t \in \mathbb{R}^+$ and a time index $n \in \mathbb{N}$. Therefore, the n-th short-time segment is $\mathbf{x}[n] = [x[n], x[n+1], \cdots, x[n+L-1]]^T$, where L is the length of the segment, i.e, $\mathbf{x}[n] \in \mathbb{R}^{L\times 1}$. Please note that in this case a rectangular window function is used as recommended in [10]. Eq. (4) can be rewritten using a matrix notation, as follows:

$$\mathbf{x}[n] = \mathbf{Z}(\phi_1[n])\mathbf{a}[n] + \eta[n] \tag{5}$$

$$\mathbf{Z}[n] = [\mathbf{e}^{j\phi_1[n]}, \mathbf{e}^{j\phi_1[n+1]}, ..., \mathbf{e}^{j\phi_1[n+L-1]}]^T \tag{6}$$

$$\mathbf{e}^{j\phi_1[n]} = [e^{j1\phi_1[n]}, e^{j2\phi_1[n]}, ..., e^{jI\phi_1[n]}] \tag{7}$$

$$\mathbf{a}[n] = [a_1, a_2, \cdots, a_I]^T \tag{8}$$

$$\mathbf{a}[n] = [A_1 e^{j\psi_1}, A_2 e^{j\psi_2}, \cdots, A_I e^{j\psi_I}]^T \tag{9}$$

where $\mathbf{Z}(\phi_1[n]) \in \mathbb{C}^{L\times I}$ or shorted $\mathbf{Z}[n]$ is a Vandermonde matrix that has the non-linear exponential complex base, the amplitudes are $\mathbf{a}[n] \in \mathbb{C}^{I\times 1}$, being $\{A_i\}_{i=1}^I$ the set of real value magnitudes, $\{\psi_i\}_{i=1}^I$ the set of real value initial phases, and $\eta[n] \in \mathbb{C}^{L\times 1}$ is stationary AWGN. The STNLS method alongside the model described on Eqs. (5) to (9) are used to estimate the IAS, please note that as stated in [11], under the assumption of AWGN, the NLS method is equivalent to the maximum likelihood method. Consequently, the NLS is a maximum likelihood estimator for the considered model for the vibration signal. The estimation of the IAS is as follows:

$$\hat{\phi}_1[n] = \underset{\{\phi_{1k}[n]\}_{k=1}^K}{\arg\min} \|\mathbf{x}[n] - \mathbf{Z}(\phi_{1k}[n])\mathbf{a}[n]\|^2 \tag{10}$$

[3] the signal is complex in range for convenience to make use of the analytic signal in practice

[4] the simplest window function will be used on this work, i.e, the rectangular function $\Pi\left(\frac{t-t_c}{t_T}\right)$, a function centred at t_c with duration t_T, and a height of 1.

Eq. (10) has as argument $\phi_{1k}[n]$, where k here is the index of the set for the optimization problem not the k-th harmonic family. As baseline it will be assumed the IAS in a short-time segment to be constant, i.e. $\phi_1[n] = \beta_2[n]$, as in [11]. But this estimation has a main limitation, the compromise between the length of the segment L, the sampling period Δt, and the IAS bounded interval $f_1(t) \in [f_1, f_2]$. Attempting to relax the aforementioned constraints and to deal with a low SNR, it is proposed a linear model for $\phi_1[n] = \sum_{n \in N} f_1[n]\Delta t$, given the segment $\mathbf{x}[n]$:

$$\phi_1[n] = \beta_1 n^2/2 + \beta_2 n \tag{11}$$
$$= \beta_1[n] + \beta_2[n] \tag{12}$$

where β_1 is the quadratic term and β_2 an initial phase for the given segment, as a consequence the Eq. (10) is rewritten as:

$$\hat{\phi}_1[n] = \underset{\{\beta_{1,k_1}[n], \beta_{2,k_2}[n]\}_{k_1,k_2=1}^{K_1,K_2}}{\arg\min} \|\mathbf{x}[n] - \mathbf{Z}(\beta_1[n], \beta_2[n])\mathbf{a}[n]\|^2 \tag{13}$$

In order to simplify the notation the dependence on the IAS and the n-th time segment are removed from the matrix $\mathbf{Z}$, for the two cases two matrices are introduced, for the constant case $\mathbf{Z}_1[n] = \mathbf{Z}(0, \beta_2[n])$, and the linear approximation case $\mathbf{Z}_2[n] = \mathbf{Z}(\beta_1[n], \beta_2[n])$. To solve the optimization problem in the Eqs. (10) and (13) it is necessary to remove the dependence of the amplitudes $\mathbf{a}[n]$, to do so, a projection is done through its least squares estimation:

$$\hat{\mathbf{a}}_i[n] = (\mathbf{Z}_i[n]^H \mathbf{Z}_i[n])^{-1} \mathbf{Z}_i[n]^H \mathbf{x}[n] | i = 1, 2 \tag{14}$$

after removing the amplitude dependence algorithmic strategies are introduced to solve the optimization problem in Eqs. (10) and (13), it has to be noted that as it is a Non-Linear problem the immediate solution it is an exhaustive search building the set of possible solutions $\{\beta_{1,k_1}[n], \beta_{2,k_2}[n]\}_{k_1,k_2=1}^{K_1,K_2}$ and to choose the $\arg\min$. The two models for $\phi_1[n]$ and some further constrains to have faster convergence will be examined in the Section 3.

2.2 REB highlight: a short-time/angle SK filtering approach

Before introducing the proposed filtering scheme, let us model a REB fault. A REB Fault at constant IAS can be modelled as a superposition of periodic impulses, where T is the period of the fault frequency, i.e., the average time between impacts, the model is proposed in [12] as follows:

$$x(t) = \sum_{i=1}^{I} A_i s(t - iT - \tau_i) + \eta(t) \tag{15}$$

where $\{A_i\}_{i=1}^{I}$ is the set of real value amplitudes, $\{\eta(t)\}_{t \in \mathbb{R}}$ is AWGN as in the previous model (see Eq. (1)), the difference lies in the function $s(t)$ that models an impact and $\{\tau_i\}_{i=1}^{I}$ is a random process to introduce small variations in the period T, in the case of *time-varying IAS* the period is no longer constant is time-varying consequently, a time-dependent function $\bar{T}(\phi_1(t)) = \phi_1(t) - iT - \tau_i$ should be introduced to explain the influence of the IAS in the REB failure vibration signal. Consequently, the variation in the IAS can be seen as a Parametrization of $x(t)$. Consequently, a REB time-varying failure signal can be written as:

$$y(t) = \sum_{i=1}^{I} A_i s[\bar{T}(\phi_1(t))] + \eta(t) \tag{16}$$

where the function $\bar{T}(\phi_1(t))$ controls the time-varying fault period making the signal cyclo-nonstationary. In contrast, a typical cyclo-stationary signal is the model in Eq. (15). Therefore, it is necessary to transform the signal $y(t)$ to be as close as possible to $x(t)$, i.e, a vibration signal at constant speed. In practice the operation to arrive from $y(t)$ to $x(t)$ is performed through uniform angular re-sampling named also computed order tracking (COT) a technique described in [5]. Traditionally, in the literature of COT it is assumed to have $y(t)$, a signal

with a time-varying IAS, the signal in angular domain is $y(\Theta)$ which is similar to $x(t)$, i.e, a version of $y(t)$ where the IAS is constant, more precisely is equal to 1. Due to a vibration signal with an IAS of 1Hz it is equivalent to have the vibration signal in rotations, i.e, in angular domain.

An important identity of the angular domain is that in the case of constant speed it is trivial to see that if the speed is the unity, i.e, $\phi_1(t) = t$ then $y(t) = x(t)$, so considering any constant speed scenario in practice the angular re-sampling is not necessary, even more, the influence of the speed is nothing more than a scale in the time and/or frequency axis, considering a simple example be $y(\gamma)$ a signal in angular domain for $\phi_1(t) = ct$ the angular domain variable is $\gamma = ct$, the operation is inversely proportional (the orders $\Gamma = \frac{1}{c}f$) in frequency domain. After the COT the time axis is termed angular domain, and its frequency domain order domain.

In general the model is only valid after filtering the impulsive behaviour of the signal due to a REB failure under variable IAS is present the vibration signal in practice is a superposition of the two used models Eqs. (4) and (16), for such a reason if a REB failure scenario is considered is mandatory to consider a filtering step to highlight the failure. The most common filter is based on the SK, consequently, a brief description of the SK will be given in the next subsection.

2.2.1 Short Time/Angle SK

To deal with a signal with a time-varying IAS the angular domain is a mandatory step, consequently, the most general approach is to first transform the signal to the angular domain, for such a reason, let us assume that the signal $x[n]$ is in the angular domain regardless if the speed is constant or time-varying. Let us consider a L length segment $\mathbf{x}[n]$, being this the n-th segments of a signal $x[n]$ with more than L point, this notation of an n-th segment is mandatory to make the estimation of the SK. Usually the consideration of segments is given per se, due to it is necessary to compute the estimation of the spectral order monments for the SK, but in the present work the distinction is made due to it is assumed that the angle-varying structural response will produce an Angle-varying SK. Consequently, the SK will be computed per n-th segment, consequently an estimator based on the Short Time Fourier Transform (STFT) of the n-th segment for the SK (a detailed definition can be found on [6]), given a window function $w(n)$, and a time lag m is introduced. Let us define the STFT of $x[n]$ as:

$$\mathrm{STFT}_x[m, f_n] := \sum_{n=0}^{L} x[n]w[n-m]e^{-j2\pi f_n} \tag{17}$$

Based on this definition, the SK can be estimated through the second and fourth order empirical spectral moment of $\mathrm{STFT}_x[m, f_n]$ defined as:

$$\hat{S}_{2x}[f_n] := \left\langle |\mathrm{STFT}_x[m, f_n]|^2 \right\rangle_m \tag{18}$$

$$\hat{S}_{4x}[f_n] := \left\langle |\mathrm{STFT}_x[m, f_n]|^4 \right\rangle_m \tag{19}$$

being $\langle\cdot\rangle_m$ the average operator through the index m. The SK is finally defined utilizing its second and fourth order empirical moment as:

$$\mathrm{SK}[f_n] = \frac{\hat{S}_{4x}[f_n]}{\hat{S}^2_{2x}[f_n]} - 2 \tag{20}$$

Please note that $\mathrm{SK}[f_n]$ is the SK for the n-th segment of length L, for such a reason let us note the SK of the n-th segment as $\mathrm{SK}_n[f_m]$. As the model in Eq. (16) is a superposition of impulses it is necessary to use second-order moments to isolate the fault frequency, but those second-order moments are conditioned to a constant speed and stationary vibration signals, for such a reason to work with the signal in the angular domain is mandatory. The most common descriptor when dealing with REB failures is the spectral correlation, a bi-spectrum which average in frequency is equal to the envelope spectrum, a brief description is made in the following subsection for a more detailed explanation view [12].

2.2.2 Envelope analysis & spectral correlation

The relationship between the traditional envelope spectrum and the spectral correlation can be summarized as the equivalence between the spectrum of cyclic frequencies $M_x(\alpha)$, i.e., the spectrum obtained integrating the spectral correlation function $S_z(\alpha, f)$ through the frequency axis f, and the envelope spectrum

$\mathrm{F}_{t\to f}\{\mathbb{E}\{|z(t)|^2\}\}$, where $z(t)$ is the analytic signal[5] of $x(t)$ being $|z(t)|^2$ the squared envelope of $x(t)$. As the spectral correlation is the double Fourier transform of the auto-correlation function, let us define the auto-correlation function for a zero mean signal $z(t)$ as:

$$R_z(t,\tau) := \mathbb{E}\{z(t+\tau/2)z^*(t-\tau/2)\} \tag{21}$$

then the spectral correlation is defined as:

$$S_z(\alpha,f) = \underset{\tau\to f}{\mathrm{F}}\left\{\underset{t\to\alpha}{\mathrm{F}}\{R_z(t,\tau)\}\right\} \tag{22}$$

The procedure for the proof is straightforward, the main result used is that the signal is dominated by its stochastic part then $R_z(t,0) = \mathbb{E}\{|z(t)|^2\}$. With the definition given in Eq. (22) and its integral across the frequency axis, the relationship between the envelope spectrum and the spectral correlation function is:

$$\begin{aligned} M_z(\alpha) &= \int_{\mathbb{R}} S_z(\alpha,f)df && (23)\\ &= \underset{t\to\alpha}{\mathrm{F}}\{R_z(t,0)\} && (24)\\ &= \underset{t\to\alpha}{\mathrm{F}}\{\mathbb{E}\{|z(t)|^2\}\} && (25)\end{aligned}$$

the previous Eq. (24) is obtained making use of the Fubini's theorem and the definition of spectral correlation (view Eq. (22)). The Eq. (25) comprises the desired relationship, thus, the integral of the spectral correlation through the frequency axis is equal to the traditional envelope spectrum. Nevertheless, the envelope spectrum can be hard to read due to the noise that masks the impulsive behaviour, such behaviour could be highlighted making use of the SK. Yet the SK is designed for stationary processes and a high time-varying IAS will produce a non-stationary signal even in angular domain, consequently, a short-time/angle filtered envelope spectrum estimation procedure is proposed in the next subsection.

2.2.3 Short Time/Angle Filtered Envelope Spectrum: welch's based estimation

Before introducing the estimation of the squared envelope spectrum using the proposed Short Time/Angle SK (STSK), it is mandatory to highlight the impulsive behaviour to be as close as possible to the model given by Eq. (15), so, for a n-th segment of length $L \in \mathbb{N}$ of a real signal in angle domain noted as $\mathbf{x}[n] = [x[n], x[n+1], \cdots, x[n+L-1]]^T$, let us consider a filtered version using the SK as:

$$\mathbf{x}_{\mathrm{SK}}[n] = \underset{f_m\to n}{\mathrm{DFT}^{-1}}\{\mathbf{X}_n[f_m]\mathrm{SK}_n[f_m]\} \tag{26}$$

where $\mathbf{X}_n[f_m] := \mathrm{DFT}_{n\to f_m}\{\mathbf{x}[n]\}$ being $\mathrm{DFT}_{n\to f_m}\{\cdot\}$ the Discrete Fourier transform of a given signal, and $\mathrm{DFT}^{-1}{}_{f_m\to n}\{\cdot\}$ the inverse Fourier transform, it should be pointed out that the Eq. (26) in practice is a filter that makes use of the convolution theorem due to a convolution in time is a product in frequency. The result is a filtered n-th segment where the impulsive behaviour is highlighted, afterwards the envelope spectrum is estimated grounded on the Welch's method of periodograms as follows:

$$\hat{S}_{|\mathbf{z}_{\mathrm{SK}}|^2}[f_m] = \frac{1}{NU}\sum_{n=1}^{N}\left|\underset{n\to f_m}{\mathrm{DFT}}\{|\mathbf{z}_{\mathrm{SK}}[n]|^2\}\right|^2 \tag{27}$$

where $\mathbf{z}_{\mathrm{SK}}[n]$ is the analytical signal, a signal whose modulus is approximately the envelope[6] of $\mathbf{x}[n]$ for a detailed explanation on how good the approximation is given in [13], and $U = \sum_{n=1}^{L}|w[n]|^2$ is the energy of the window. The result is a short-angle filtered approximation of the envelope spectrum noted $\hat{S}_{|\mathbf{z}_{\mathrm{SK}}|^2}[f_m]$. Which it is expected to produce an improvement of the SNR, given that the proposal has an optimal angle-variant SK filter (angle-frequency 2D), using the Welch's method of periodograms in short segments that makes the computation of the filtered envelope spectrum faster with respect to the traditional approaches in the state of the art.

[5] an analytic signal is a signal without negative frequencies where $z(t) := x(t) + j\mathscr{H}\{x(t)\}$ being $\mathscr{H}\{\cdot\}$ the Hilbert transform.

[6] the instantaneous envelope and phase are well defined only for mono-component signal, then is advisable to pre-filter $z_k(t)$ in order to have a mono-component signal.

3 Experimental set-up

Two experiments are proposed, one in a numerical dataset and a case study of an aircraft engine, for both the numerical and the case study, the IAS is estimated employing the proposed STNLS and a fault in REB is highlighted by the 2D short-angle filter STSK. The robustness of the IAS STNLS estimator will be studied under the influence of two types of Noise, Pink and Additive White Gaussian Noise (AWGN). The robustness test is made only in a numerical case, due to, only in a numerical signal, the SNR can be controlled. For the proposed STSK filter, the REB highlighting is compared against two methodologies, a naive approach and the traditional state of the art approach. Regarding the case study, the IAS estimation is compared against the reference signal measured from the tachometer signal, and for the failure in a REB, a visual comparison is made as well as for the numerical case.

3.1 Numerical test: IAS estimation & REB highlight

Usually the models in the state of the art for time-varying IAS does not take into account the effect of the transfer function, consequently, to have a more realistic and challenging signal it is introduced the transfer function $h[n]$ in the model presented in the Eq. (4) as follows:

$$\hat{x}[n] = h[n] \circledast \sum_{i=1}^{I} a_i[n] e^{j\phi_i[n]} + \eta[n] \tag{28}$$

where $\circledast(\cdot,\cdot)$ represents the convolution operator between two functions, an example of the numerical signal with the influence of the transfer function as stated in the Eq. (28) is shown in the Fig. 1, to be even more challenging the signal presents a random discontinuity in all the orders comprised by a piecewise formulation, i.e., the amplitudes $a_i[n] = 0$ for all $i \in I$ and for all n in an interval $[n_1, n_2] \subset [0, L]$, where $n_1 \approx 2.5$fs and $n_2 = n_1 + 0.1$fs. In this case the interval is of 0.1sec, such discontinuity is as misleading for any IAS tracking algorithm as an impulse, like the one produced by a REB failure.

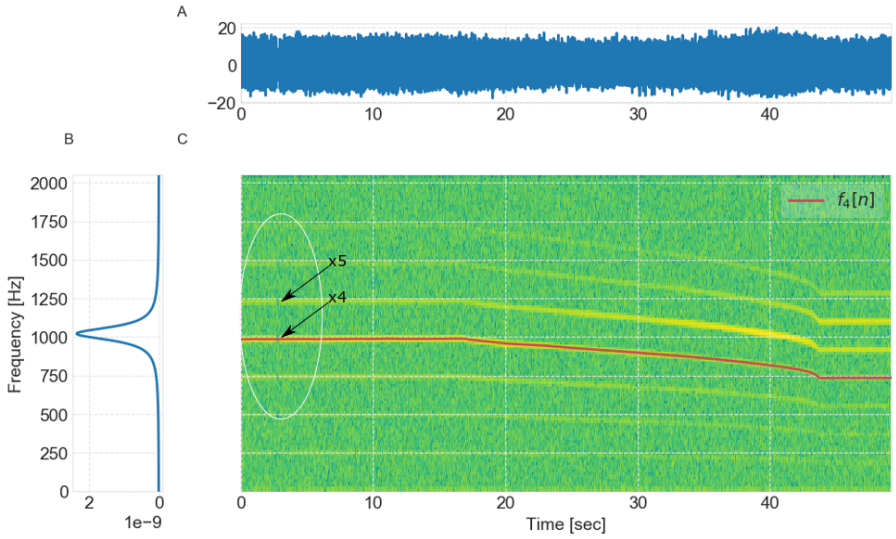

Figure 1: Numerical signal with AWGN of 3dB, a) in time, b) transfer function $H(f)$, c) spectrogram showing a random discontinuity of 0.1 sec reflected on all orders.

The considered sampling frequency fs is of 2^{12} samples per second, and the signal is contaminated with AWGN to accomplish a SNR of 3dB, also in order to be as realistic as possible the IAS $\phi_r[n]$ is from the real case study described in Section 3.2, only that the time indexes are compressed by a factor of 4, i.e., the used IAS $\phi_1[n] = \phi_r[4n]$. The compression is done for computational reasons.

3.1.1 IAS estimation: robustness test

In order to prove the robustness of the proposed IAS estimation methodology the numerical signal in the Eq. (28) will be contaminated with different levels of AWGN and Pink noise[7] with a SNR in the interval $[-10,10]$dB, and as baseline it is considered the IAS estimated with a null quadratic term, i.e., $\beta_1[n]=0$, as measure of estimation error it is used the Mean-Squared-Error (MSE), which is defined as:

$$\text{MSE}\{f_1[n],\hat{f}_1[n]\}=\frac{1}{N}\sum_{n=1}^{N}|f_1[n]-\hat{f}_1[n]|^2 \tag{29}$$

where $\hat{f}_1[n]\in\mathbb{R}^N$ is the estimated IAS, and $f_1[n]$ the real IAS profile for the entire signal of length N, being being $N>L$, and L has as length the amount of samples equivalent to 0.2sec. Recalling the minimisation problem in the Eq. (13) a minimisation algorithm should be used but as there is no an explicit Jacobian, the Nelder-Mead algorithm is selected. The parameters of the algorithm are: an initialization value ($\{\beta_{1,nd}[0],\beta_{2,nd}[0]\}$), the optimization function that will produce an scalar value using the logarithmic version of the Eq. (13) for a faster convergence. The amount of orders I, conditioned by the sampling frequency (all the possible orders are considered), and a tolerance for the convergence of 10^{-6}. The initialisation is made through the minimum of the cost function using a grid for the first segment $n=0$; nevertheless, the problem is non-convex as shown in the Fig. 2, for such a reason the initialisation is of extreme importance due to the functional to optimize could fall into a suboptimal solution.

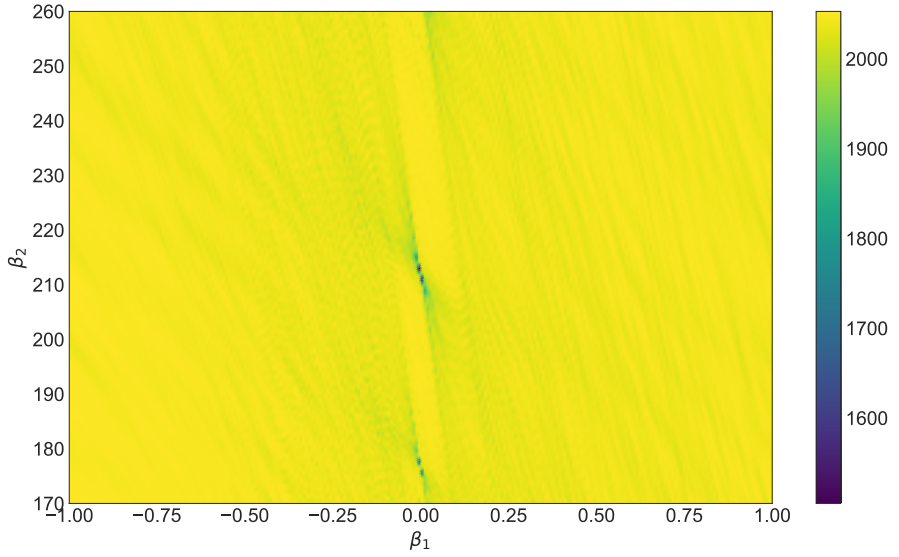

Figure 2: Cost function in the Eq. (13) for a segment of the the exemplary signal in Fig. 1 at 35sec.

As the optimisation is made per segment, it is assumed that the IAS does not variates significantly from the n-th segment with respect to the $n+1$-th segment, so after the initialization using the cost function, the parameters are initialized as $\beta_{i,nd}[n+1]=\hat{\beta}_i[n]$ for $i=1,2$ for $n>0$.

The resulting estimated parameters $\hat{\beta}_1[n]$, and $\hat{\beta}_2[n]$ for the piecewise estimation (for each n-th segment) for the robustness test ($[-10,10]$dB of SNR) are shown in the Figs. 3 and 4 for the AWGN and Pink Noise case respectively, alongside with the reconstruction of the IAS $\hat{f}_1[n]$ by means of the Eqs. (11) and (12) for the entire signal. The reconstruction is made taking into account that it is used an overlap of half of the points $L/2$. It should be noticed that when the quadratic term $\beta_1[n]$ is null the linear term $\beta_2[n]$ is in fact the IAS, being the IAS the derivative of the phase and the derivative of $\beta_2 n=\beta_2$ per each n-the segment. where the n in $\beta_2 n$ could take values from $[n+1,n+L-1]$. As can be seen in Figs. 3 and 4 all the estimations are superposed for different levels of noise where each colour represents a SNR level.

In the Fig. 3 is shown that the AWGN is the worst kind of noise to be expected, due to its presence in the whole spectrogram, meanwhile the estimation in the Fig. 4 contaminated with Pink Noise it is almost perfect due to the noise is decreasing with respect to the frequency, making the harmonic model extremely robust

[7] where the Pink Noise is defined in terms of its Power Spectral Density (PSD) as $\eta_{\text{PN}}[f_m]\approx 1/f_m$.

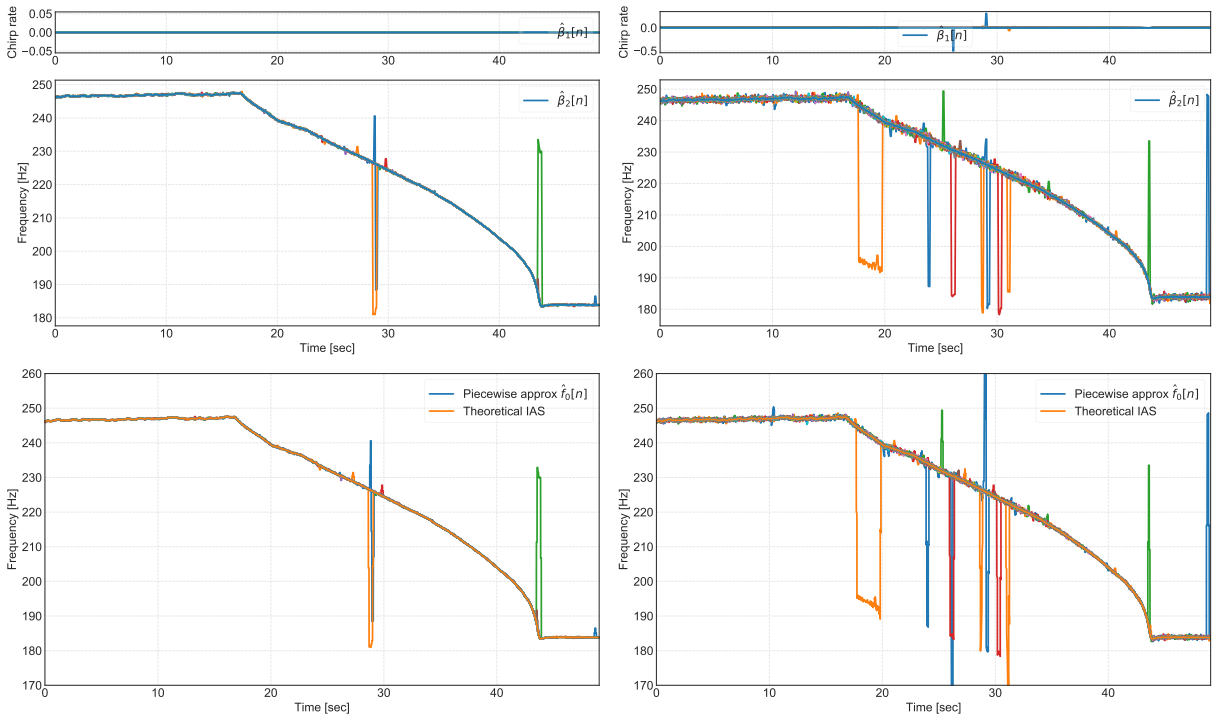

Figure 3: AWGN test, first-column:$\beta_1[n]$, $\beta_2[n]$, and IAS estimated no linear approximation, second-column: $\beta_1[n]$, $\beta_2[n]$ and IAS estimation after linear approximation, for all the considered signal polluted with noise in to achieve a for SNR in $[-10, 10]$dB.

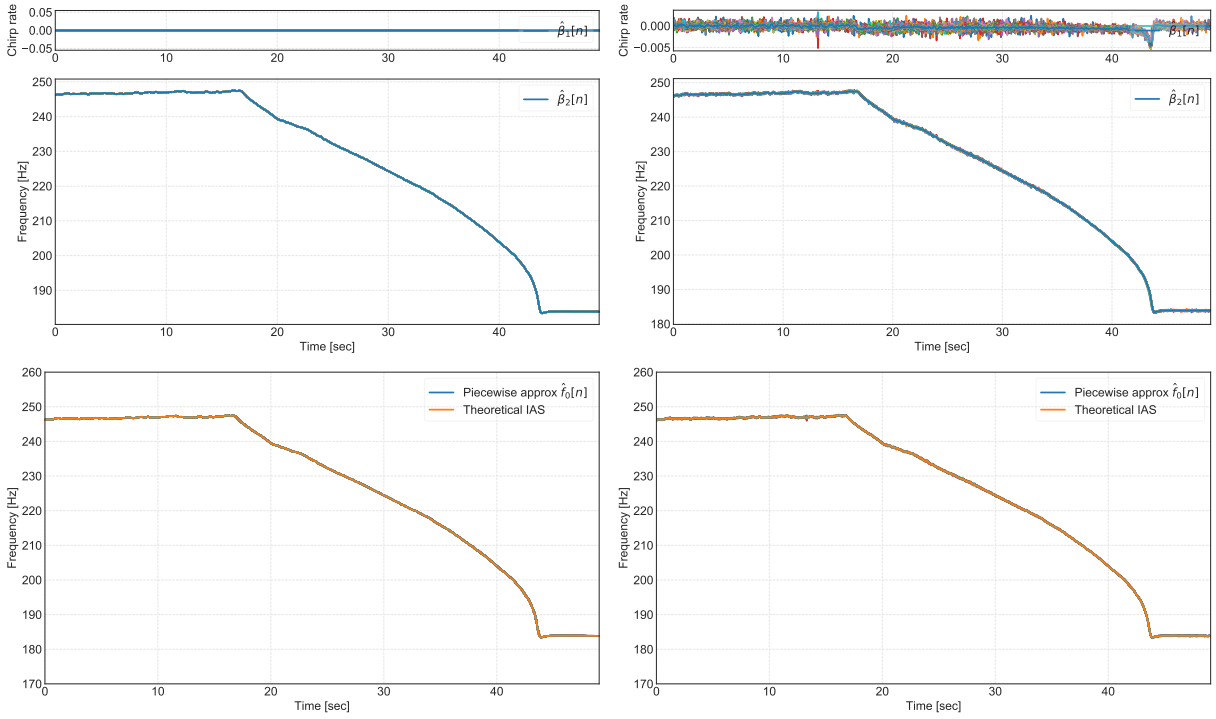

Figure 4: Pink noise test, first-column:$\beta_1[n]$, $\beta_2[n]$, and IAS estimated no linear approximation, second-column: $\beta_1[n]$, $\beta_2[n]$ and IAS estimation after linear approximation, for all the considered signal polluted with noise in to achieve a for SNR in $[-10, 10]$dB. Figure to compare with the Fig. 3

to Pink Noise. The Fig. 3 shows that for the AWGN case are two critical segments the one that comprises the segment with the discontinuity of 0.1sec around 30sec and the segment where the speed has the highest variation at 45sec.

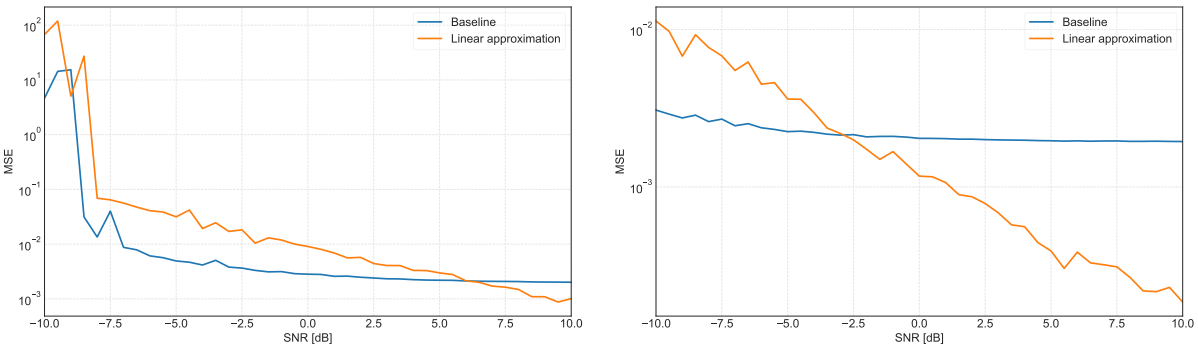

Figure 5: SNR vs MSE tests for an SNR between $[-10, 10]$dB, in the left the AWN scenario, and in the right the Pink-noise scenario, for the baseline and linear IF reconstruction of the IAS $\hat{f}_1[n]$ using Eqs. (11) and (12)

The Fig. 5 shows the MSE for the baseline, and the linear approximation for the two types of considered noise, as expected a decreasing behaviour of the MSE by respect the SNR is shown, for both the baseline and the linear approximation. Nevertheless, the linear approximation of the IAS with low SNR, i.e, less than 6dB for AWGN and -3dB for Pink Noise, is worst with respect to the baseline (quadratic term null). Due to the introduction of the quadratic term (the slope of the IAS) amplifies the errors at low SNR, in contrast with a good SNR improves the estimation. It should be pointed out that there are misleading errors (peaks in Figs. 3 and 4) those errors could be erased with an additional filter, like a median filter, yet it is not part of the scope of the work and taking into account the challenging theoretical signal, the results are encouraging, experimentally proving the robustness of the parametric methods.

3.1.2 REB failure detection

As it is not defined an standard scalar bearing fault indicator, the fault detection is usually made through visual examination for such a reason it will not be considered an SNR test in this subsection. The numerical signal in the Fig. 6 is modelled using the Eq. (16). The signal simulates a Ball Pass Frequency Inner-race (BPFI) fault with a fault frequency (with period T) of 5.875Hz, with a linear IAS profile creasing from 5Hz to 60Hz and contaminated with AWGN to achieve a SNR of 3dB.

The signal in time, the IAS profile, and its spectrum is shown in Fig. 6, as it is expected from the visual examination of the spectrum of the considered bearing fault, a second-order descriptor like the envelope spectrum should be used. Furthermore, as the speed variates the angular domain transform is a mandatory step. The resulting filtered envelope spectrum through the proposed STSK filtering approach are shown in Fig. 7, where the only parameters for the STSK are the size of the windows: for the computation of the standard SK is of 4096 samples and a larger window for the Short-angle SK of 65536 samples given a sampling frequency of 512 samples per revolution.

The Fig. 7 shows a comparison between two baseline methodologies and the STSK proposed approach, initially it is assumed a naive approach that does not take into account that the transfer function $h(t)$ (LTI) becomes angle-variant (Non-LTI), so the vibration signal $x[n]$ is re-sampled to the angular domain and after the state of the art SK filtering and posterior envelope spectrum estimation. With this naive approach the first fault harmonic x1 is almost destroyed. The second approach is to isolate with the SK the impulsive band, i.e, the frequency band with highest SK, assuming that the signal filtered by the SK is close to the model in the Eq. (16). This approach gives the expected decreasing spectrum, but surprisingly the highest energy is located in the second harmonic of the fault frequency x2. Finally, the proposed STSK approach is summarized in the Eq. (27) which is short-time/angle based, as it is short-angle based the transfer function will remain LTI, and the failure is better highlighted due to the SK filter is optimal segment based, i.e, each segment will follow the model Eq. (16), as result the first harmonic of the failure x1 is dominant and there is a decreasing distribution of the energy for the rest of the harmonics, making the failure highly diagnosable visually examining the filter

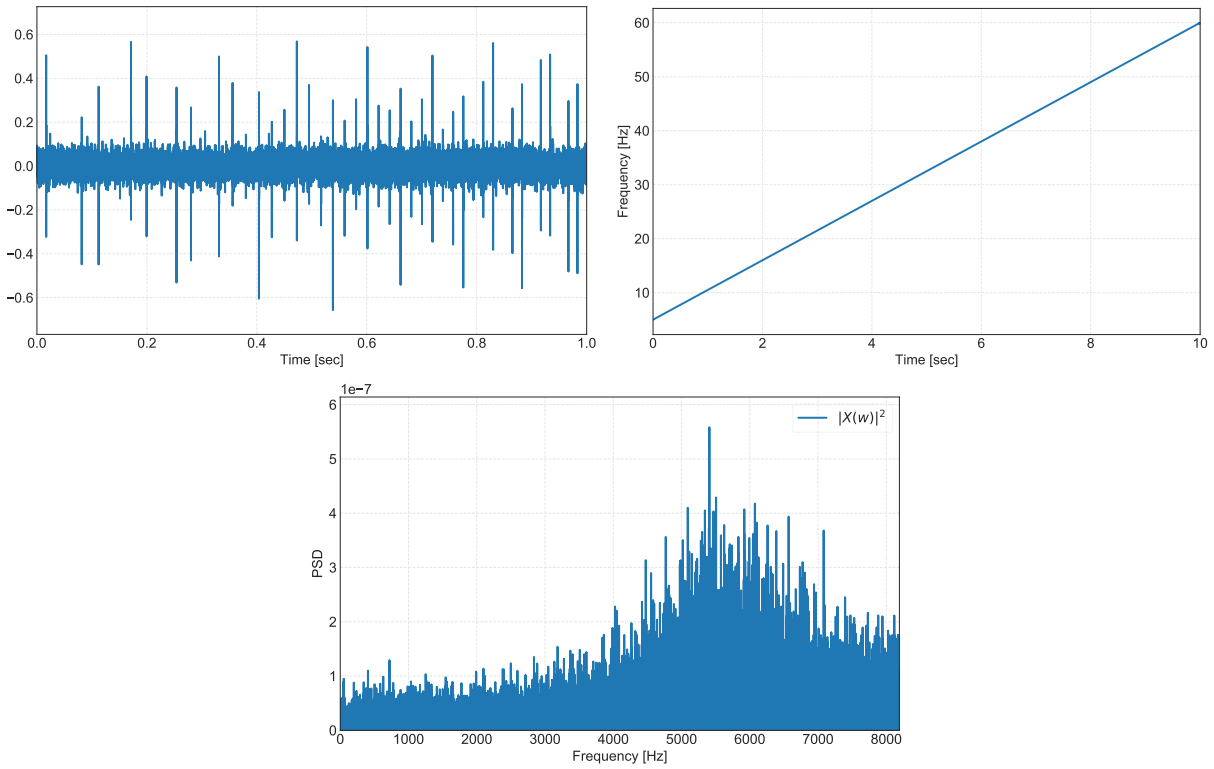

Figure 6: Top-row: left) numerical signal in time with a BPFI at 5.875Hz, right) IAS profile, bottom-row: spectrum of the simulated signal.

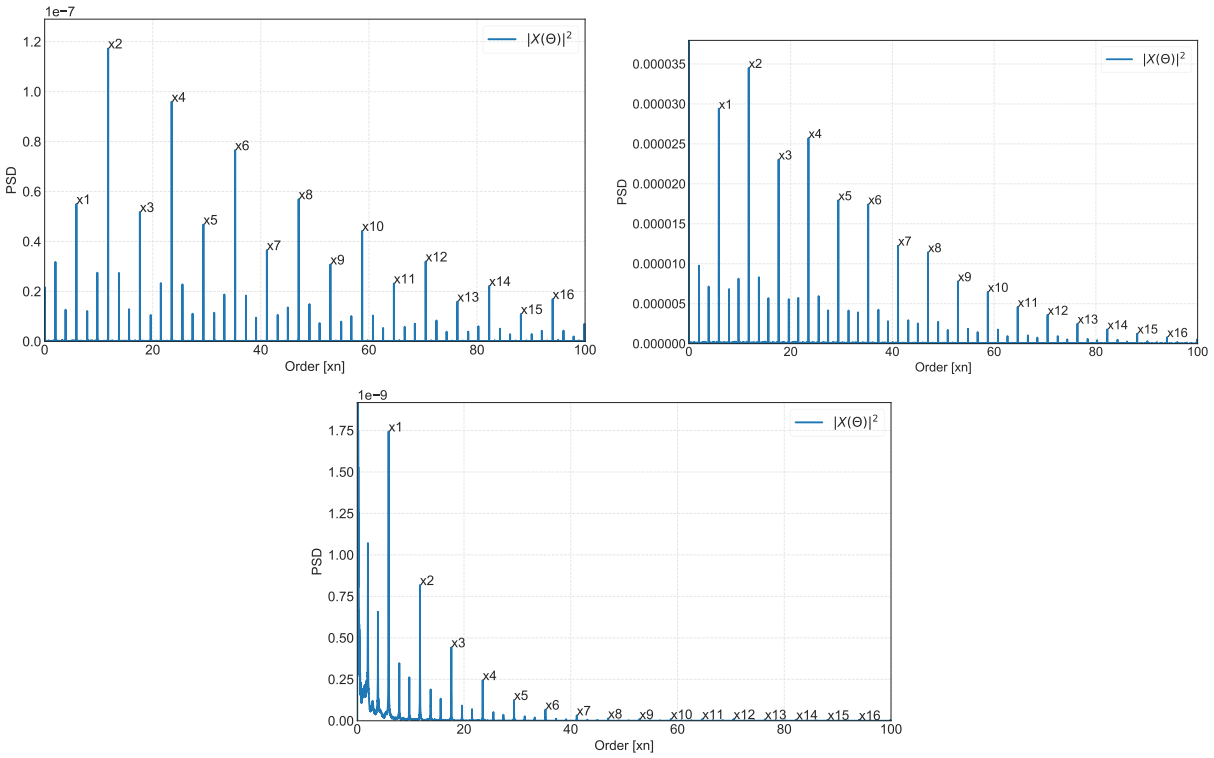

Figure 7: Top-row: baseline methodologies, left) angular domain transform, SK filtering, then envelope spectrum, right) SK filtering, angular domain transform, then envelope spectrum, bottom-row: proposal) angular domain transform, then, envelope spectrum convolved with a time-frequency dependent SK based filter.

envelope spectrum.

3.2 Case study: an aircraft engine

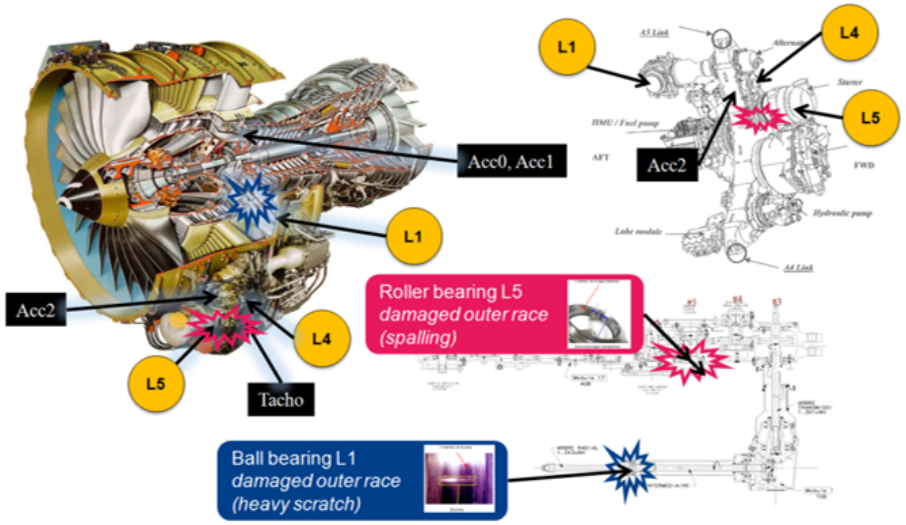

Figure 8: General overview of the engine and the accessory gearbox. Shafts (L1-L5) are identified by labels in amber colour (image taken from [4]).

The data was acquired during a ground test on a civil aircraft engine. The Fig. 8 gives a general overview of the engine with the damaged bearings and the sensors locations. The engine has two main shafts and an accessory gearbox with pieces of equipment such as pumps, filters, alternators, and starter. The accessory gearbox is linked to the high-pressure shaft HP by a radial drive shaft and a horizontal drive shaft. The records have a sampling frequency of 50kHz, it should be noted that the fault it is only in the record ACC2, and it is taken close to L5, for such a reason it is expected to view mainly the fault in outer race of that line, also, as there are several lines, L5 is chosen as reference for the fault frequencies, the table with the fault frequencies referenced to L5 are shown in Table 1. For a more detailed explanation (kinematics) of the dataset and the recorded signals please refer to [4].

	L1(L5)	L4(L5)	L5(L5)
Speed	1,34	0,984	1
Cage	0,55	0,40	0,43
Rolling element	3,46	2,44	3,56
Inner race	7,95	5,87	10,24
Outer race	5,45	3,97	7,76

Table 1: Table of fault frequencies of bearings for the supporting shafts L1, L4, L5, taking as reference the speed of L5.

3.2.1 IAS estimation

The short-time estimation of the IAS has only as critical parameter the window size L and the overlap is $L/2$, the window size is two times the period of the minimum expected frequency of 170Hz, there are have two records to study ACC1 normal condition and ACC2 with a fault. The spectrograms of the records are shown in Fig. 9, in the left column it is shown the signals with the entire frequency spectrum from 0 to 25kHz, and in the right the signals with a down-sampling of 16 times. For the record ACC2, it is not expected to extract accurately the IAS due to, the information from the down-sampled record is almost destroyed by the transfer function of the structure, i.e., a redistribution of the energy to a high-frequency band. A typical phenomenon when dealing

with bearing failures. For such a reason it makes more sense to extract the highest energy harmonic, that is the one related with the amount of teeth for gear located at L5, i.e., the harmonic 62 of the IAS.

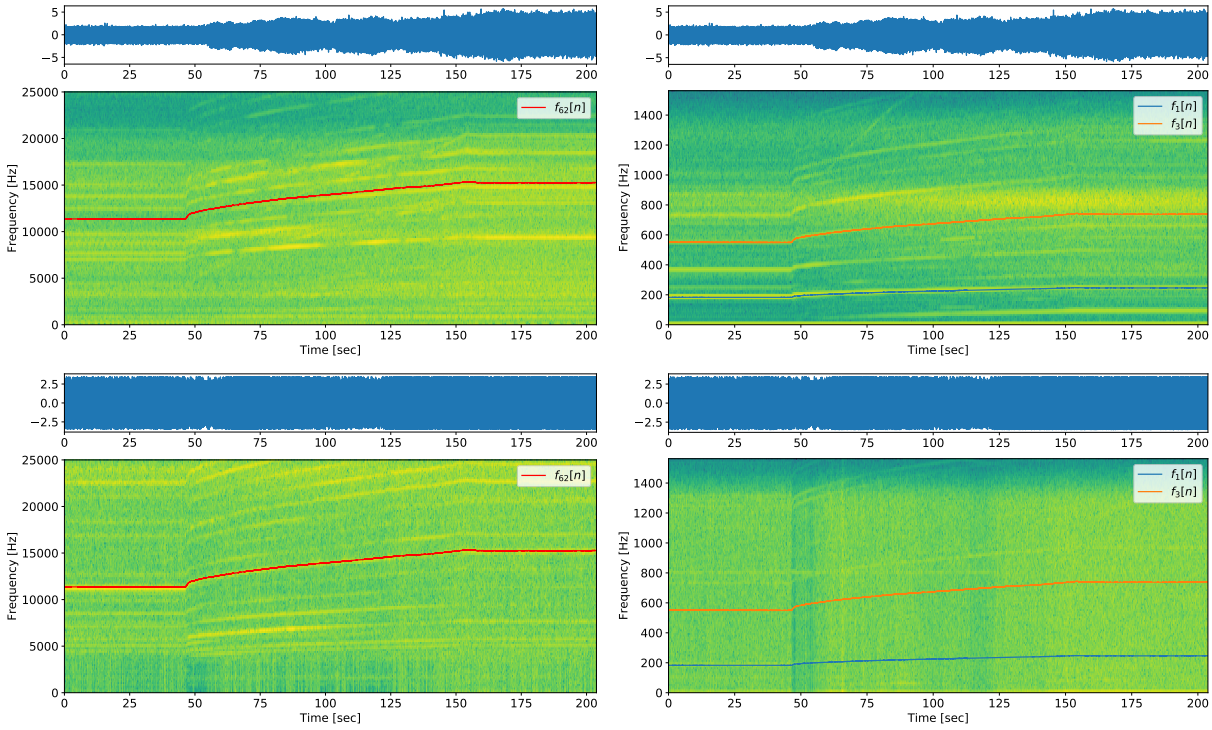

Figure 9: Top-row: spectrograms ACC1, left, full frequency range $[0,25]$kHz, right, down-sampled to $[0,1.56]$kHz, bottom-row: spectrograms for ACC2 same frequency ranges than in top figures.

As it is expected in the Fig. 10 is shown that the STNLS method is not able to extract the IAS from the ACC2, in contrast, the IAS extracted from the ACC1 is a perfect match visually comparing the IAS obtained from the tachometer signal, and the one obtained employing the proposed methodology. In terms of MSE the IAS obtained through the proposed piece-wise linear approximation is of 4.93×10^{-3} and 14.56×10^{-3} for the proposed methodology with and without quadratic term β_1 respectively. Similarly, without down-sampling the corresponding MSEs are: 2.15×10^{-3} and 2.94×10^{-3}, the improvement in the MSE it is expected, due to there are more points to compute the cost function. The results are consistent concerning the numerical test where it is verified that the influence of the quadratic term could introduce errors when dealing with low SNR.

As in the previous experiment Fig. 10 the IAS was not successfully extracted for the ACC2 record, consequently, the most natural approach is to extract the highest energy harmonic $\times 62$ after the visual examination of the Fig. 9, as a result it is shown in the Fig. 11 that the proposed methodology could extract the IAS even from a challenging record. Yet the results are far from the ones obtained for the record ACC1. Being the MSE for the record ACC2 of 3.21 and 3.19 for the estimation without and with the inclusion of the quadratic term β_1 respectively.

The critical point is after 50sec where the estimation partially lost the optimal point, and followed a sub-optimal as previously analysed in the numerical cost function in Fig. 2 the optimization problem is not convex and prone to fall into a sub-optimal. That point is critical disregard the inclusion of the quadratic term, for such a reason the IAS extraction on a record under a REB failure at high variable speed such as ACC2 continues to be a subject of research.

3.2.2 REB failure detection

In this subsection is done the angular re-sampling with the signal from the tachometer to not to bias the experiment, the signal was recorded located on HP tacho (L4), and the ACC2 record the only record with the bearing failure. In order to filter the vibration signal to obtain a signal as close as possible to the model Eq. (16), the experiment is the same as the previously done in the Section 3.1.2. As a result there are three scenarios to highlight the REB failure: first the naive approach, then, angular re-sampling, then SK filtering,

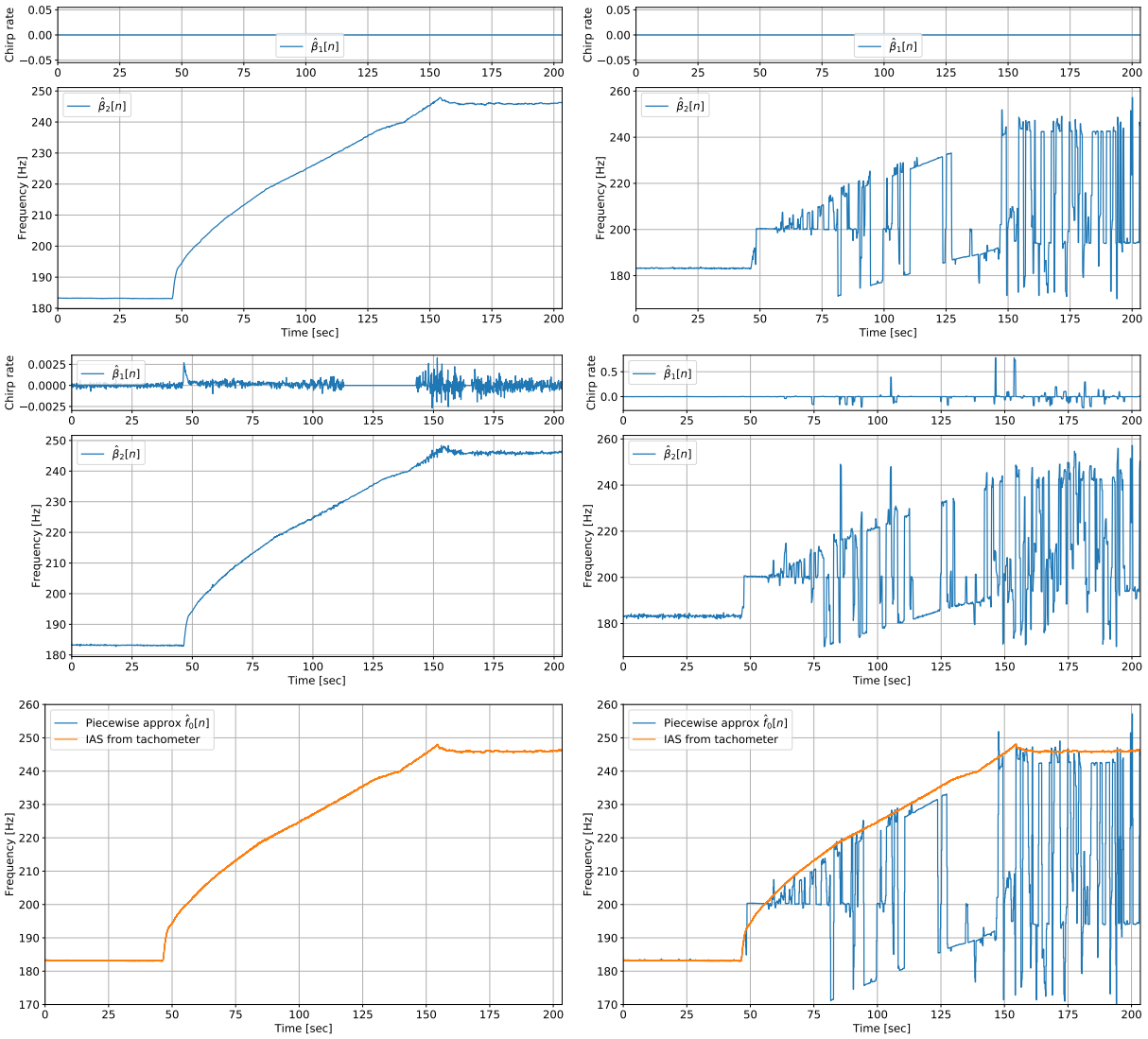

Figure 10: Left-column ACC1, right-column ACC2, rows: i) phase estimation without linear approximation, ii) phase with linear approximation $\{\beta_i[n]\}_{i=1}^{2}$, iii) IAS estimation after linear approximation.

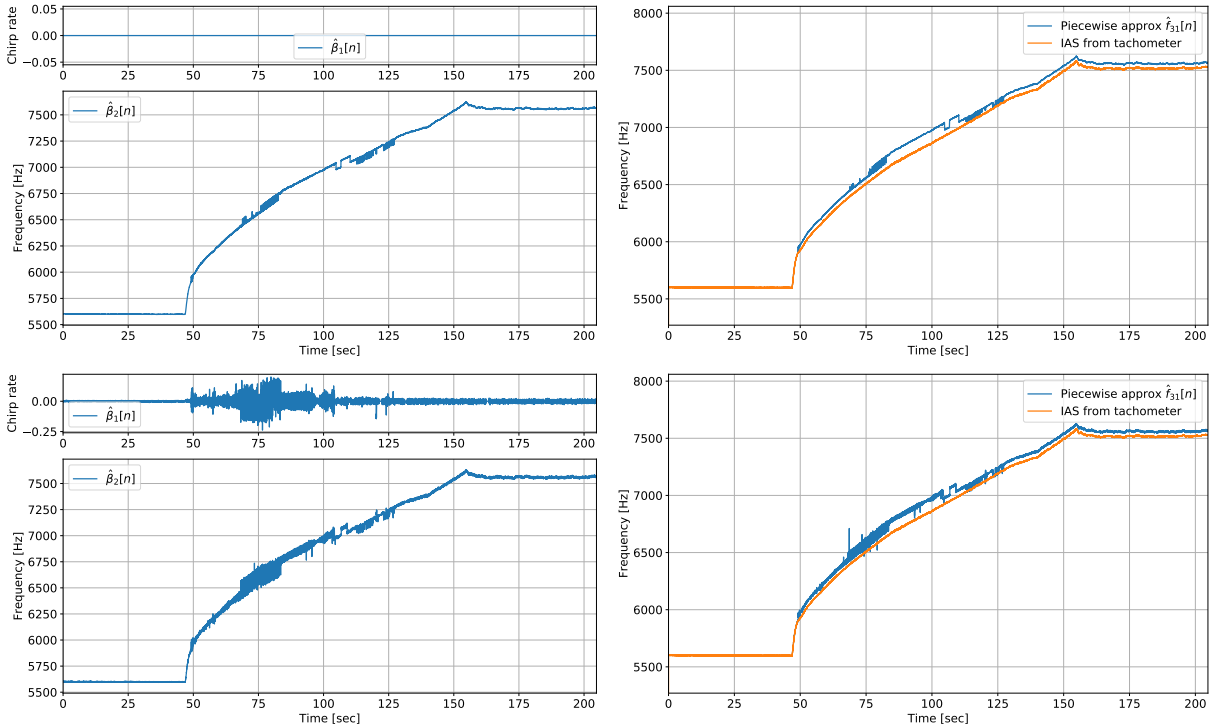

Figure 11: ACC2: IAS estimation approximation taking as fundamental frequency $f_{31}[n]$, top-row: without linear approximation, bottom-row: with linear approximation.

then envelope spectrum, the state of the art approach) SK filtering, then angular re-sampling, the envelope spectrum (valid only for small variations on the IAS), and finally the proposed approach short-angle based the STSK, angular re-sampling the short-angle SK based filter and the envelope spectrum obtained by means of the Welch's method of periodograms (filtered periodograms).

The results of the three considered scenarios are shown in the Fig. 12, where it is made a zoom close to the fault frequency 7.68evp (events per revolution). For the naive approach there is no highlight of the energy in the fault frequencies, for the traditional state of the art method the fault is highlighted, yet, the spectrum is noisy due to the SK is conceived for stationary signals a condition that is not fulfilled, given the significant variation of the IAS. Finally with the proposed STSK method the failure is highlighted and now appears some side-bands corresponding to half of the cage failure frequency of the other bearing failure in L1 a failure that only is made present with the proposed approach. The method is not sensible to the parameters, due to the only parameters necessaries are the window for the short angle SK (a larger window than the one of the SK itself), and a window for the SK computation itself (SK computation is based on the STFT). The first window is the next power of 2 of the period of the smallest expected frequency (131072 samples), and the window for the computation of the SK is 4096 samples, given a sapling frequency of 256 samples per revolution.

4 Conclusion

In the present work, a REB failure identification methodology under variable IAS is proposed, two tasks are addressed, the IAS failure estimation and the impulsive behaviour filtering for failure identification. Due to the fact that IAS introduces non-stationarities assuming that a signal in a short time window is highly stationary (cyclo-stationary), short-time/angle approaches are proposed for the two tasks at hand. For the proposed STNLS IAS estimation technique a robustness test is done building a database of contaminated signals with AWGN and Pink Noise and measuring the MSE between the theoretical IAS and its estimation for different levels of Noise. Also, to corroborate the methodology in a real scenario, the IAS is successfully retrieved from two records from an aircraft engine under a failure in REB. The second contribution is a short-angle SK filtering approach (STSK) to highlight the impulsive behaviour that has the information related to the failure. The proposed STSK is tested in a numerical signal and the aircraft engine, successfully highlighting the fault frequencies, and

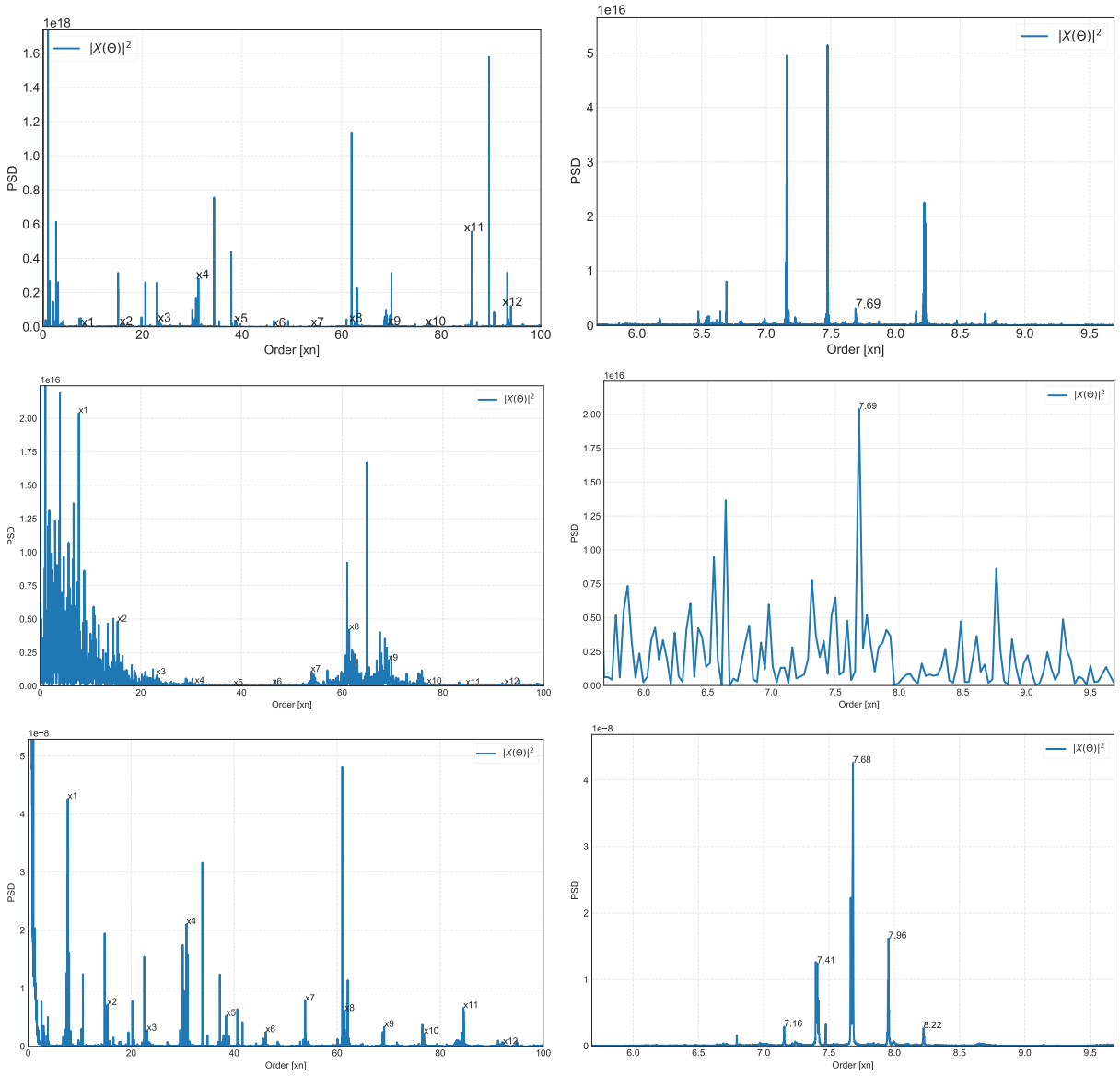

Figure 12: Top-row: baseline one, angular domain transform, SK filtering, then envelope spectrum, Middle-row: SK filtering, angular domain transform, then envelope spectrum, Bottom-row: **proposal** angular domain transform, then, envelope spectrum convolved with a time-frequency dependent SK based filter.

outperforming the traditional methodologies of the state of the art. As future work it will be interesting to study another parametric approaches for IAS estimation like the particle filter and polynomial Fourier transform. The algorithms are publicly available in https://github.com/efsierraa.

Acknowledgements

This work was performed within the framework of the Labex CeLyA of Université de Lyon, operated by the French National Research Agency (ANR-10-LABX-0060/ANR-11-IDEX-0007), the Convocatoria 647 de 2014 de Colciencias-Colfuturo, and IDEX-LYON "aide á la mobilité internationale des doctorants".

Références

[1] Randall, R.B., Antoni, J. : Rolling element bearing diagnostics - a tutorial. Mechanical Systems and Signal Processing 25(2), 485–520 (2011)

[2] Zimroz, R., Urbanek, J., Barszcz, T., Bartelmus, W., Millioz, F., Martin, N. : Measurement of instantaneous shaft speed by advanced vibration signal processing-application to wind turbine gearbox. Metrology and Measurement Systems 18(4), 701–712 (2011)

[3] Leclère, Q., André, H., Antoni, J. : A multi-order probabilistic approach for instantaneous angular speed tracking debriefing of the cmmno 14 diagnosis contest. Mechanical Systems and Signal Processing 81, 375–386 (2016)

[4] Antoni, J., Griffaton, J., André, H., Avendaño-Valencia, L.D., Bonnardot, F., Cardona-Morales, O., Castellanos-Dominguez, G., Daga, A.P., Leclère, Q., Vicuña, C.M., et al. : Feedback on the surveillance 8 challenge : Vibration-based diagnosis of a safran aircraft engine. Mechanical Systems and Signal Processing 97, 112–144 (2017)

[5] Fyfe, K., Munck, E. : Analysis of computed order tracking. Mechanical Systems and Signal Processing 11(2), 187–205 (1997)

[6] Antoni, J. : The spectral kurtosis : a useful tool for characterising non-stationary signals. Mechanical systems and signal processing 20(2), 282–307 (2006)

[7] Randall, R., Sawalhi, N., Coats, M. : A comparison of methods for separation of deterministic and random signals. International Journal of Condition Monitoring 1(1), 11–19 (2011)

[8] Borghesani, P., Ricci, R., Chatterton, S., Pennacchi, P. : A new procedure for using envelope analysis for rolling element bearing diagnostics in variable operating conditions. Mechanical Systems and Signal Processing 38(1), 23–35 (2013)

[9] Abboud, D., Baudin, S., Antoni, J., Rémond, D., Eltabach, M., Sauvage, O. : The spectral analysis of cyclo-non-stationary signals. Mechanical Systems and Signal Processing 75, 280–300 (2016)

[10] Christensen, M.G., Jensen, J.R. : Pitch estimation for non-stationary speech. In : 2014 48th Asilomar Conference on Signals, Systems and Computers. pp. 1400–1404. IEEE (2014)

[11] Christensen, M.G., Jakobsson, A. : Multi-pitch estimation. Synthesis Lectures on Speech & Audio Processing 5(1), 1–160 (2009)

[12] Randall, R.B., Antoni, J., Chobsaard, S. : the Relationship Between Spectral Correlation and Envelope Analysis in the Diagnostics of Bearing Faults and Other Cyclostationary Machine Signals. Mechanical Systems and Signal Processing 15(5), 945–962 (sep 2001), http://linkinghub.elsevier.com/retrieve/pii/S0888327001914153

[13] Picinbono, B. : On instantaneous amplitude and phase of signals. IEEE Transactions on Signal Processing 45(3), 552–560 (1997)